[CANCER RESEARCH 56, 3091-3102, July 1, 1996]

Genetic Alterations in Untreated Metastases and Androgen-independent Prostate Cancer Detected by Comparative Genomic Hybridization and Allelotyping[1]

Michael L. Cher,[2,3] G. Steven Bova,[2] Dan H. Moore, Eric J. Small, Peter R. Carroll, Sokhom S. Pin, Jonathan I. Epstein, William B. Isaacs, and Ronald H. Jensen

Departments of Urology [M. L. C., P. R. C.], Laboratory Medicine [R. H. J], Hematology Oncology [E. J. S.], and Biostatistics [D. H. M.], University of California School of Medicine and University of California, San Francisco/Mt. Zion Medical Center, San Francisco, California; and Departments of Urology, Pathology and Oncology [G. S. B., S. S. P., J. I. E., W. B. I.], Johns Hopkins University School of Medicine, Baltimore, Maryland

ABSTRACT

A newly developed method of comparative genomic hybridization (CGH) employing quantitative statistical comparisons was applied to DNA from two different types of advanced prostate cancer tissue. Multiple CGH analyses were obtained for each chromosome in each tumor, and the results of point-by-point comparison of the mean tumor:normal color ratio to a control normal:normal color ratio in each of 1247 evenly distributed data channels constituting the entire human genome were interpreted as loss, gain, or no change in copy number in the tumor genome. Group I tissue was obtained from prostate cancer metastases from 20 patients, 19 of whom had received no prior prostate cancer treatment. This DNA also was analyzed by Southern and microsatellite allelotyping at 53 different loci on 20 different chromosome arms. CGH results agreed with allelotyping results at 92% of the informative loci studied. These samples, which contained highly enriched tumor DNA, showed the highest rates of alteration yet reported in several chromosomal regions known to be altered frequently in prostate cancer: 8q gain (85%), 8p loss (80%), 13q loss (75%), 16q loss (55%), 17p loss (50%), and 10q loss (50%). Group II tissue was obtained predominately from primary or recurrent tumor from 11 patients who had been treated with long-term androgen-deprivation therapy and developed androgen-independent metastatic disease. Quantitative CGH analysis on DNA from these tissues showed chromosomal alterations that were very similar to those found in group I, suggesting that untreated metastatic tumors contain the bulk of chromosomal alterations necessary for recurrence to occur during androgen deprivation. In the entire data set, a number of previously undetected regions of frequent loss or gain were identified, including losses of chromosomes 2q (42%), 5q (39%), 6q (39%), and 15q (39%) and gains of chromosomes 11p (52%), 1q (52%), 3q (52%), and 2p (45%). χ^2 analysis showed a significantly higher frequency of gain of the 4q25-q28 region in tumors from African-American patients, indicating a possible oncogene whose activation may play a role in the higher rate of progression seen in this ethnic group. Additional study of these frequently altered regions may provide insight into the mechanism of prostate cancer progression and lead to important tools for tumor-specific prognosis and therapy.

INTRODUCTION

Molecular genetic mechanisms responsible for the development and progression of prostate cancer remain largely unknown. Identification of sites of frequent and recurring allelic deletion or gain is a first step toward identifying some of the important genes involved in the malignant process. Previous studies in retinoblastoma (1) and other cancers (2–4) have demonstrated amply that definition of regional chromosomal deletions occurring in the genomes of human tumors can serve as an important initial step toward identification of critical genes. Similarly, regions of common chromosomal gain have been associated with amplification of specific genes (5). Additionally, definition of the full spectrum of common allelic changes in prostate cancer may lead to the association of specific changes with clinical outcome, as indicated by recent studies in colon cancer and Wilms' tumor (6, 7).

Prostate cancer allelotyping studies (8, 9) designed to investigate one or two loci on many chromosomal arms have revealed frequent LOH[4] on chromosomes 8p (50%), 10p (55%), 10q (30%), 16q (31–60%), and 18q (17–43%). Recently, several groups have performed more detailed deletion-mapping studies in some of these regions. On 8p, the high frequency of allelic loss has been confirmed, and the regions of common deletion have been narrowed (10–15). Similar efforts have also served to narrow the region of common deletion on chromosome 16q (12, 16). Other prostate cancer allelotyping studies utilizing a smaller number of polymorphic markers have not revealed new areas of interest (17–20). At present, allelotyping studies are limited by the low number of loci studied, low case numbers, heterogeneous groups of patients, the use of tumors of low or unclear purity, and lack of standardization of experimental techniques. For these reasons, it has been difficult to compare frequencies of alterations between studies, and we have yet to gain an overall view of regional chromosomal alterations occurring in this disease.

CGH is a relatively new molecular technique used to screen DNA from tumors for regional chromosomal alterations (21). Unlike microsatellite or Southern analysis allelotyping studies, which typically sample far less than 0.1% of the total genome, a significant advantage of CGH is that all chromosome arms are scanned for losses and gains. Moreover, because CGH does not rely on naturally occurring polymorphisms, all regions are informative, whereas polymorphism-based techniques are limited by homozygous (uninformative) alleles among a fraction of tumors studied at every locus.

Previously, we showed that CGH can detect and map single copy losses and gains in prostate cancer with a high degree of accuracy when compared with the standard techniques of allelotyping (22). We and others also have generated copy-number karyotype maps for prostate cancer showing several recurrently altered regions of the genome (22, 23). These studies have begun to reveal a genome-wide view of chromosomal alterations occurring in primary and recurrent prostate cancer, but to date, metastatic prostate cancer has not been examined in depth.

In the present study, our goal was to obtain an overview of the complete array of chromosomal alterations involved in the development and progression of prostate cancer. To that end, we chose to study tumor tissues from patients with advanced disease. We applied a newly developed quantitative CGH technique to DNA isolated from a set of prostate cancer lymphatic and bony metastases. Careful dissection was used to enrich these samples for tumor cells to maximize our sensitivity in detecting alterations. The quantitative CGH analytical technique was validated by multiple Southern and micro-

Received 1/15/96; accepted 5/1/96.

The costs of publication of this article were defrayed in part by the payment of page charges. This article must therefore be hereby marked *advertisement* in accordance with 18 U.S.C. Section 1734 solely to indicate this fact.

[1] This work supported by NCI Grants CA59457, CA58236, and the Association for the Cure of Cancer of the Prostate (CaP CURE). M. L. C. was supported by the American Foundation for Urological Disease with funds provided by TAP Pharmaceuticals, Inc.

[2] M. L. C. and G. S. B. contributed equally to this work.

[3] To whom requests for reprints should be addressed, at Departments of Urology and Pathology, Wayne State University School of Medicine, 4160 John R, Suite 1017, Detroit, MI 48201.

[4] The abbreviations used are: LOH, loss of heterozygosity; CGH, comparative genomic hybridization; PSA, prostate-specific antigen.

satellite allelotyping measurements performed on the same samples. We also performed CGH on DNA extracted from a set of prostate tumors from patients with androgen-independent metastatic disease to compare the spectrum of chromosomal alterations in these tumors with those in the untreated metastatic cancers. Using this strategy, we produced genome-wide, region-specific frequency histograms for chromosomal losses and gains in prostate cancer and identified several new regions likely to contain genes important to the development and progression of this disease.

MATERIALS AND METHODS

Metastatic or primary tumor tissue was obtained from two groups of patients with metastatic prostate cancer (see Table 1). Group I consisted of 20 patients who had not been exposed to long-term androgen deprivation or other therapies. Group II consisted of 11 patients with clinical disease progression despite long-term androgen deprivation therapy (androgen-independent disease).

Group I Tissue from Metastases. Eighteen of these 20 patients were thought initially to have tumors confined to the prostate but were later found to have pelvic lymphatic metastases at the time of staging pelvic lymphadenectomy. Portions of the metastatic cancer tissue obtained at lymphadenectomy were used for this study. None of these 18 had undergone androgen deprivation therapy, chemotherapy, or radiation therapy prior to this surgery. The remaining two samples were obtained from patients with prostate cancer metastatic to the bone. One of these patients (patient 375) underwent androgen deprivation therapy 1 month prior to bone biopsy. The other patient (patient 391) received no therapy prior to bone biopsy.

Considering these 20 patients together, the mean age at the time of tissue sampling was 61 years, with a range of 44–72 years. Five of the men are of African-American descent, the other 15 are Caucasian, with no more detailed ethnic data available. Mean serum PSA (Hybritech) 1 day to 20 weeks prior to pelvic node dissection or bone biopsy for the 20 men was 61 ng/ml, with a range of 3.3–250 ng/ml. Mean prostate biopsy Gleason score (24) for the 18 men found to have pelvic metastases was 7, with a range of 4–9 (Table 1). Family history of prostate cancer was available for 12/20 patients, and was negative for all 12.

Precise histological control was achieved for all tissues studied in this group using the following protocol. Tissues not needed for histological diagnosis were snap frozen at −80°C within 10–30 minutes after surgical removal. Serial cryostat sectioning was used to identify portions of the sample containing a lower fraction of tumor cells. These areas were removed from the tissue block by microdissection every 300 μm. The area of tissue remaining after microdissection varied from approximately 2 × 5 mm to 10 × 20 mm. The estimated tumor cell fraction (fraction of the sample composed of tumor cells as opposed to lymphocytes or stromal cells) was determined by visual estimation in 20 randomly selected fields examined at total magnification of ×100 (Olympus Optical Co., Ltd., Tokyo, Japan) and averaged for all histological sections produced during serial sectioning (Table 1). DNA was obtained from between 200 and 1000–6μm sections for each case. If we estimate that one tumor cell is contained in every 1000 μm^3 tissue volume, the samples studied consisted of DNA pooled from between 10^7 and 10^9 metastatic prostate cancer cells. DNA purification was performed as described previously (10). Aliquots of the same DNA samples were used for both allelotyping and CGH. For both Southern and microsatellite analysis, noncancerous comparison DNA was prepared from pooled blood lymphocytes from each patient.

Group II Tissue from Androgen-independent Cases. These patients showed clinical disease progression despite long-term androgen-deprivation therapy. Four patients underwent transurethral resection for locally advanced tumor obstructing the bladder outlet, six patients underwent core biopsy of recurrent pelvic tumor after radical prostatectomy, and one patient suffered a scrotal skin metastasis. Thus, genetic analysis was performed on primary tumor in four cases, persistent or recurrent primary tumor in six cases, and metastatic tumor in one case.

Considering these 11 patients together, the mean age at the time of tissue sampling was 72 years, with a range of 43–96 years. All of these 11 patients are Caucasian, with no more detailed ethnic data available. Mean serum PSA at the time of diagnosis of metastatic prostate cancer was 272 ng/ml with a range of 14.9–1632 ng/ml. Mean Gleason Score was 7.6 with a range of 6–10.

Histological control was less precise for these tissues, because the estimated

Table 1 *Clinical data on patients from whom tissue was taken for analysis*

Group	Specimen number	Age	Race	Serum PSA	Primary tumor Gleason score	Tissue studied	Estimated tumor cell fraction
I	50	69	C[a]	21.0	7	LN met	0.9
	133	70	C	69.7	9	LN met	0.85
	142	61	C	26.2	9	LN met	0.95
	170	57	C	3.3	4	LN met	0.9
	259	69	C	32.3	7	LN met	0.95
	273	53	C	29.0	7	LN met	0.85
	275	66	C	123.0	6	LN met	0.65
	344	60	C	29.7	7	LN met	0.85
	375	54	C	12.0	9	Bone met[b]	0.75
	391	57	C	16.9	5	Bone met	0.95
	399	65	C	23.6	7	LN met	0.9
	402	56	C	41.3	7	LN met	0.9
	418	68	A	21.4	8	LN met	0.7
	419	57	A	102.0	5	LN met	0.95
	491	72	A	250.0	8	LN met	0.75
	497	45	C	130.0	8	LN met	0.65
	522	57	C	13.3	7	LN met	0.9
	556	66	C	9.2	8	LN met	0.85
	628	44	A	235.0	7	LN met	0.85
	635	65	A	31.0	6	LN met	0.9
II[c]	1	75	C	299.0	7	Prostate bx	unknown[d]
	2	96	C	142.0	7	TURP	0.65
	3	65	C	1632.0	9	Prostate bx	0.5
	4	67	C	14.9	7	Prostate bx	0.5
	5	75	C	209.0	9	TURP	0.9
	6	85	C	105.0	9	TURP	0.8
	7	58	C	58.8	6	Prostate bx	0.5
	8	78	C	22.0	7	Prostate bx	0.6
	9	78	C	232.0	7	Prostate bx	0.4
	10	74	C	106.0	6	Skin met	0.7
	11	43	C	173.0	10	TURP	0.95

[a] Abbreviations: C, Caucasian; A, African-American; LN, pelvic lymph node; met, metastasis; bx, biopsy; TURP, transurethral resection of prostate.
[b] Patient received 1 month of androgen-deprivation therapy prior to tissue sampling.
[c] Group II tumors progressed clinically while on androgen-deprivation therapy. For these tumors, histological analysis was performed on adjacent surgical samples.
[d] Slides could not be located.

tumor cell fraction was not determined directly on the piece of tissue from which DNA was isolated. Instead, it was estimated from a histological section of a nearby piece of tissue removed during the same surgical procedure. Thus, the estimated tumor cell fraction listed in Table 1 is less precise than for group I. DNA was isolated from fresh tissue brought immediately from the operating room or clinic by proteinase K dissection and phenol-chloroform-isoamyl alcohol extraction. Serial cryostat sectioning was not used.

CGH. CGH was performed as described previously (22) with the modification that DNA was labeled by direct incorporation of fluorochrome-linked nucleotides. Briefly, tumor DNA (0.5–1 μg) was labeled by nick translation in the presence of 20 μM dATP, dCTP, dGTP, and FITC-12-dUTP (NEN Research Products, Boston, MA). Normal DNA, isolated from the lymphocytes of a laboratory volunteer, was labeled in an identical fashion using Texas Red-5-dUTP (NEN Research Products). Hybridization with 0.2–1.0 μg of labeled tumor and normal DNA and 10 μg of Cot-1 DNA was performed on metaphase spreads from a normal donor's lymphocytes for 2–3 days, the slides were washed and dehydrated in ethanol, and the metaphase spreads were counter-stained with 0.1 μM 4′,6-diamidino-2-phenylindole.

Five to 10 fluorescence microscopic metaphase images of each color were acquired for each tumor-normal hybridization; 4 to 5 images were chosen for quantitative analysis. For each metaphase image, green (tumor) and red (normal) fluorescence intensity values were calculated as described previously (22, 25). The green and red fluorescence intensity values along each chromosome were then assigned to data channels appropriate for their location in the genome. There were 1247 data channels extending along the length of the genome from 1pter to Yqter with the number of channels for each chromosome assigned to a fixed value based on the relative lengths of the chromosomes (26, 27). Thus, channels 1–100 contained fluorescence intensities measured for chromosome 1, channels 101–197 contained intensities for chromosome 2, and so on. Each metaphase image generally yielded intensity values of each color for both members of all autosome pairs and one intensity value of each color for chromosome X and chromosome Y. Fluorescence intensity of each color was normalized for a given metaphase and the ratios of green:red were calculated for each data channel for each chromosome image. Green:red fluorescence intensity ratio distributions (means and SDs) were then calculated for each data channel, taking into account the ratios from every chromosomal image in every metaphase that was analyzed. In general, averages over 7 images of each autosome were combined (range 4–10) to provide a fluorescence intensity ratio profile distribution along the genome for each tumor.

Quantitative Analysis by CGH. To quantitatively analyze CGH data, we compared results from tumor-normal hybridizations with those from normal-normal controls. Thus, we performed five two-color hybridizations involving only normal DNA labeled both green and red to be used as controls for comparison with tumor-normal hybridizations. CGH was performed using the same methodology as that used for tumor DNA. For each of these control hybridizations, four metaphase images were analyzed, resulting in up to eight images for each autosome and four images for each sex chromosome. As expected, the green:red ratios were centered around 1.0 along the length of the genome for each of these control hybridizations. However, close examination of the ratios revealed that many genomic regions consistently showed green:red ratios slightly different from 1.0. For example, the region corresponding to chromosome 1p32–1pter showed an average green:red ratio of 1.07, the region corresponding to chromosome 19 showed an average ratio of 1.08, and the region corresponding to chromosome 4q showed an average ratio of 0.952. The cause of these consistent deviations in the green:red ratios in the normal-normal control hybridizations was unknown. We suspect that hybridization properties are altered slightly by incorporation of conjugated uridine into the probe DNA, and these hybridization differences are revealed by slight variations in particular regions of the metaphase chromosomes, perhaps because of protein/DNA interactions or chromosomal structure. Additionally, SDs of the ratios tended to vary from region to region. For example, SDs tended to increase near chromosomal telomeres and centromeres. At the centromeres, this can be explained by the fact that unlabeled Cot-1 DNA was added to block nonspecific repetitive DNA hybridization by the labeled DNAs, and because large amounts of repetitive DNA are present at the centromeres, a decreased intensity of both green and red fluorescence resulted in these regions. The decreased intensity of both fluorescence colors resulted in lower precision in the intensity measurements and ratio calculations. At the telomeres, there appears to be a slight uncertainty in the definition of the exact terminus as determined by the image analysis algorithm because there is a large area of local background that causes local decrease in the chromosomal image intensity for both colors. As with the centromeric regions, this resulted in a lower precision in intensity measurements at the telomeres.

Data from these five control normal-normal hybridizations, obtained under the same experimental conditions as for the tumor-normal hybridizations, were combined to model the behavior of the ratios when no genetic alterations were present. Therefore, each of the 1247 data channels along the genome in the control hybridizations was assigned a specific green:red fluorescence intensity ratio distribution. We then compared the green:red distributions for each tumor-normal hybridization to those for the combined pool of control normal-normal hybridizations. A t statistic was calculated independently for each channel along the genome to test whether the mean ratio for a tumor-normal hybridization was significantly different from the mean ratio for the control normal-normal hybridizations. Derivation of this t statistic is described in Moore *et al.* (28). At each of the 1247 data channels, larger absolute values of t indicated higher statistical confidence that a chromosomal alteration was truly present. Positive values of t indicated gain of genetic material in the tumor DNA, whereas negative values of t indicated loss of genetic material. Finally, centromeric and heterochromatic regions were excluded from interpretation, because hybridization in these regions is imprecise (25).

In quantitative CGH analysis, a threshold t value must be chosen to use the t statistic for defining whether a ratio at any point along the genome indicates a significant gain or loss of genetic material in any given tumor DNA sample. The value of the threshold directly affects the sensitivity and specificity of CGH analysis and should be set according to the goals of the study. To define this threshold for our study, we calculated the t statistics for each of the normal-normal control hybridizations by comparing each one to the complete set of five control hybridizations. During this analysis, we found that smoothing the normal-normal ratio variances by averaging over several contiguous channels prior to formation of the t statistic greatly reduced the number of false "gains" and "losses" in the control hybridizations. Thus, we adopted this procedure for all our t-statistical calculations, and the variance in each data channel for the normal-normal elements in the analysis was averaged with those of five contiguous channels on each side of that channel. Within five channels of chromosomal termini and centromeres, the number of contiguous channels in this averaging was decreased systematically by averaging only to the terminus or centromere. Using this procedure for t-statistical evaluation, the t values for all of the control hybridizations were near 0, with very few elevated positive or negative values (Fig. 1). For example, 99% of t values for the control hybridizations were between −1.36 and 1.36. For this study, we

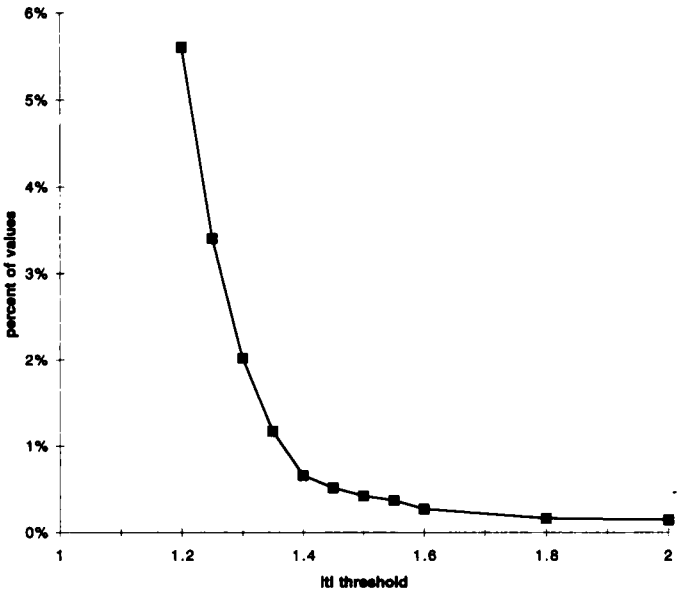

Fig. 1. Setting the t threshold based on control, normal-normal hybridizations. For five control hybridizations, each with 1247 t values extending along the genome from 1pter to Yqter (a total of 6235 t values), the Y axis gives percentage of t values with absolute value greater than the given threshold on the X axis.

chose a threshold of $|t| > 1.6$ for the definition of losses and gains. At this threshold level less than 0.3% (17 out of 6235) $|t|$ values from the five normal-normal control hybridizations were over the threshold. On the basis of the curve shown in Fig. 1, lowering the t threshold would result in a rapid loss of specificity (*i.e.*, would increase false positives); also, this threshold level resulted in a high level of sensitivity for the detection of chromosomal alterations based on the high level of concordance with the independently performed allelotyping experiments (see "Results").

Allelotyping. For the 20 group I metastatic tumors, Southern analysis was carried out at 29 loci on 19 chromosome arms, and microsatellite analysis was performed at 24 loci on 7 arms. Many of the loci were chosen because they fell within regions found previously to be relevant to prostate cancer. In particular, we tested multiple loci on the following chromosome arms (chromosome arm, number of loci compared): 2q, 3; 8p, 9; 10q, 5; 13q, 12; 16q, 5; and 18q, 3. In addition, 12 other chromosome arms were represented with one or two loci each.

Loci studied by Southern analysis were *D1S57, D1S74, D2S44, D2S48, D2S50, D2S53, RAF1*(3p), *D4S125, D6S44, D7S150, KSR* (8p), *MSR* (8p), *D8S140, D8S220, D8S194, D8S39, IFNB1* (9p), *D10S25, D10S28, D13S1, D13S2, D16S7, CETP-A/B* (16q), *TAT* (16q), *D17S5, D17S34, D17S74, DCC* (18q), and *DYZ4* (Y). Southern analysis was performed as described previously (10).

Loci studied by microsatellite analysis were *D2S123, APC* (5q), *D8S201, LPL* (8p), *D8S261, D8S264, D10S190, D10S192, D10S201, D10S217, D13S115, D13S121, D13S134, D13S146, D13S147, D13S152, D13S170, D13S171, D13S175, D13S309, D16S26, D16S402, D18S61*, and *D18S69* (29). Microsatellite analysis was performed as described previously (10).

Allelic loss using Southern and microsatellite analysis was defined as the absence of one allele in prostatic tumor DNA compared to the noncancerous paired control DNA as determined by inspection of the autoradiograph. In some cases, when there was residual signal from contaminating normal tissue, densitometry was used for analysis. A sample was scored as having allelic loss if approximately 60% reduction was present in the diminished allele compared to its normalized retained counterpart.

Only one region (chromosome 8q) showed allelic gain by Southern blotting. Allelic gain using probe *MCT 128.2* (8q) was defined as an increase in intensity of greater than 100% of one of two alleles present in tumor samples, or intensity differences of greater than 100% between tumor and normal alleles in homozygous cases when prior probing of the same blots demonstrated equal loading of DNA in tumor and normal lanes. Allelotyping measurements were performed and analyzed in a blinded fashion with respect to the CGH findings.

RESULTS

Hybridization Quality. We found that the direct labeling technique of incorporation of fluorochrome-linked nucleotides into genomic DNA resulted in higher-quality hybridization when compared with the older technique of detection using fluorochrome-linked secondary reagents (22). By fluorescence microscopic examination, this increase in quality could be seen as less granular images with sharper transitions of color at the termini of losses and gains. Additionally, image analysis tracings of the fluorescence ratios were smoother, such that when data from multiple images were combined, the SDs of the fluorescence ratios were reduced.

CGH Using t Threshold 1.6. On all tumor DNA samples, we applied quantitative CGH as described in "Materials and Methods," using t thresholds of $+1.6$ for gains and -1.6 for deletions. With this analytical approach, all tumors in both groups of specimens displayed some DNA alterations (gains or deletions relative to average DNA copy number). The proportion of the genome with either gains or deletions was calculated separately for each tumor and is depicted in Fig. 2. It is clear that a large fraction of the genome appears altered in most specimens. Thus, the high level of specificity obtained by using $|t| > 1.6$ did not sacrifice the sensitivity to detect changes. Samples displayed different relative proportions of gains and losses, with no specific pattern among samples in each group. Overall, there were nearly equal proportions of the genome involved in gains as in losses; group I averaged 15% of genome gained and 14% lost, and group II averaged 16% gained and 11% lost.

As a test of the reproducibility of this new CGH method, one tumor DNA sample was submitted and analyzed twice in a blinded fashion. Using the t statistic method, regions of loss and gain were determined independently on these two specimens. DNA from this particular tumor (tumor 50) showed a large number of alterations, with 26% of the genome showing a significant gain and 21% of the genome showing a significant loss. In comparing the results of the two independent analyses, 89% of the 1247 data channels indicated identical locations for gains, losses, or no change. The primary differences in the two data sets are at the termini of alterations, where t values are changing rapidly with channel number. An illustration of this comparison is shown in Fig. 3, where the t values in the data channels for chromosome 10 from each of the two runs are plotted, and the t thresholds are indicated. In this illustration, both the relative agreements and disagreements can be viewed. The two data sets agree in 46 (84%) of 55 data channels, with the majority of the differences occurring in small regions (one or two contiguous channels). This duplicate determination illustrates the power of CGH to present reproducible locations of gains and losses over the entire genome and also displays its weakness as a lack of high resolution in defining the location of alterations.

We also compared this quantitative statistical approach to the previous method of interpretation using simple green:red ratio threshold analysis. In the past, green:red ratio thresholds of 1.2 and 0.8 have been used commonly for delineation of gains and deletions, respectively (22). At these thresholds, the simple green:red ratio analysis agreed with the t statistic analysis ($|t| > 1.6$) at 78% of data channels over all 31 tumors. Of the discordant data channels, 99% occurred in situations where $|t| > 1.6$, but the green:red ratio analysis showed no alteration. Taken together with the high level of concordance with allelotyping described below, these data demonstrate the increased

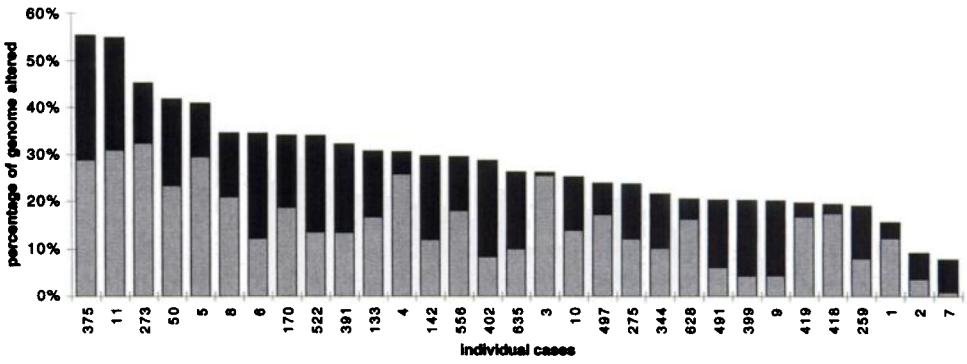

Fig. 2. Percentage of the genome with alterations. The percentage of the genome gained (*shaded bars*) and deleted (*solid bars*) as determined by $|t| > 1.6$ is plotted for each tumor specimen.

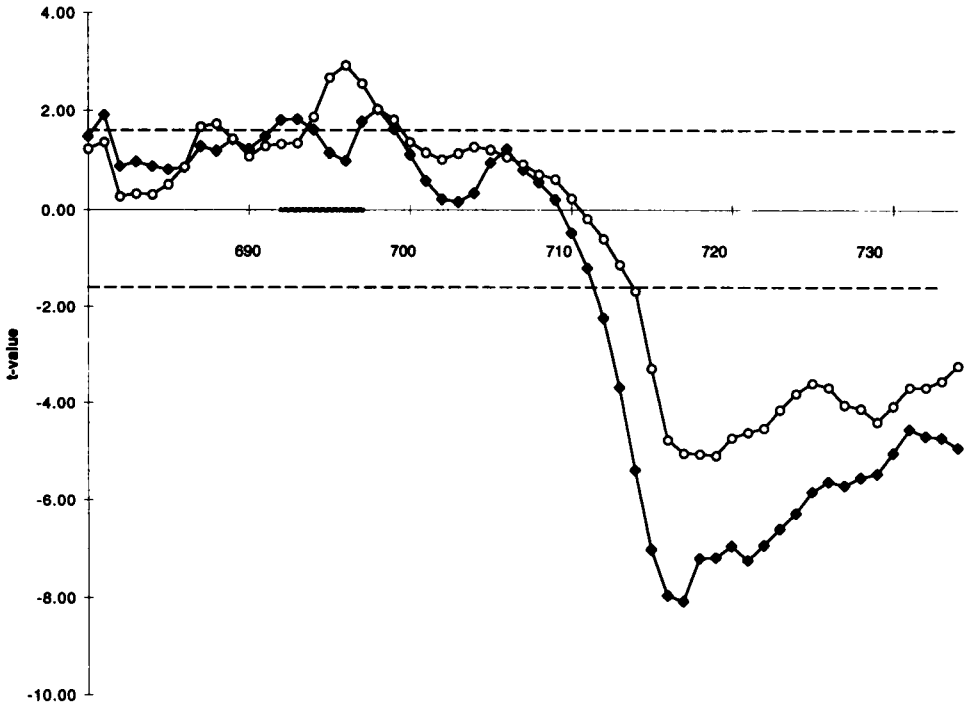

Fig. 3. Comparison of two CGH analyses on a single DNA specimen. One tumor DNA specimen was analyzed by CGH analysis two times in a blinded fashion. The entire CGH procedure, including labeling, hybridization, and analysis, was performed independently for each specimen. *t* values for the 55 data channels of chromosome 10 for the first and second analysis are depicted by the circles and diamonds, respectively. A threshold of 1.6 is shown by *dotted lines*. *X axis*, data channel number (of 1247 total); *heavy line between channels 690–700*, region of centromere.

sensitivity and specificity gained by application of the quantitative statistical analysis.

CGH Concordance with Allelotyping. To validate this quantitative statistical approach to CGH analysis, we compared CGH with allelotyping results on each of the 20 group I tumor specimens. Fig. 4 shows an example of the method of comparison for two tumors on one chromosome.

Overall, the allelotyping studies resulted in 280 informative results at 49 different loci. A summary of the comparisons to CGH is shown in Table 2. Of the 280 informative results obtained with allelotyping, 44 instances could not be compared to CGH because of imprecise physical mapping of the Southern probes or microsatellite polymorphisms relative to the termini of CGH-defined alterations. Of those that could be compared, discordant results occurred in only 18 of 236. Twelve of these 18 disagreements occurred in instances where CGH indicated a loss but the alleles appeared balanced. The level of agreement using the κ statistic (30), which takes into account agreement that might occur by chance alone, is $\kappa = 0.83$ (95% confidence interval is 0.70–0.95), with no difference in the level of agreement of CGH with Southern or microsatellite analysis.

Frequency of Regional Chromosomal Alterations: Group I. To define the general tendencies of DNA alterations in the genome of untreated tumor metastases, we created a point-by-point histogram along all chromosome arms showing the region-specific frequency of losses and gains in this series of 20 untreated prostatic metastases. Fig. 5 shows the frequency of occurrence of $|t| > 1.6$ for each data channel plotted relative to an ideogram of each chromosome. The following nine chromosomal arms showed loss (in at least one region of each arm) in more than 40% of the cases: 8p (80%), 13q (75%), 16q (55%), 2q (50%), 10q (50%), 17p (50%), 5q (45%), 6q (45%), and 15q (45%), and the following seven chromosomal arms showed gain (in at least one region of each arm) in more than 40% of the cases 8q (85%), 1q (55%), 11p (55%), 2p (50%), 3q (45%), 7q (45%), and 9q (45%), as shown in Fig. 5.

Close examination of the frequency histograms in Fig. 5 reveals that some of the frequently altered regions contain smaller subregions with higher frequencies of alteration than adjacent regions. For example, losses on chromosome 13 increase in frequency continuously from 13q11–q21.1, remain at about 70% through 13q21.1–q22, and decrease continuously in frequency from 13q22 to q35. Thus, the region 13q21.1–q22 displays the highest chance of containing an important prostate tumor suppressor gene. Detailed analysis of such regions with a technique of higher resolution (such as PCR microsatellite allelotyping) is required to define the region more precisely.

Fig. 5 shows other chromosomal regions that are altered in a somewhat lower proportion of group I tumors. The most frequent of these are 3p gain (40%), 4p gain (40%), and 11p loss (30%). Interestingly, there are 12 chromosomal arms where both losses and gains were detected in at least 20% of the cases. In 7 of these 12 arms, the regions of loss and gain do not overlap, and it could be that recessive and dominant oncogenes are distributed throughout these regions. Again, more precise localization of each region would address this question better.

Finally, Fig. 5 shows a modest frequency of alterations (5–20%) in almost all areas of the genome, suggesting that some clonal chromosomal alterations arise randomly and are maintained in proliferating prostate cancer cells.

Frequency of Chromosomal Alterations: Group II. Eleven specimens from patients with disease progression despite long-term androgen deprivation also were analyzed by CGH. As with group I specimens, we performed a point-by-point histogram analysis along all chromosomal arms showing the region-specific frequency of alterations. Overall, the results revealed a pattern of chromosomal alterations very similar to those that were seen for DNA isolated from group I tissues. In particular, the most commonly detected changes were a loss in chromosome 8p, a gain in chromosome 8q, and a loss in chromosome 13q. Histograms obtained for these chromosomes of group II samples (Fig. 6) appear quite similar to those obtained for group I (Fig. 5). To test for differences in chromosomal alterations between group I and group II specimens, we constructed 2 × 3 contingency tables at each of the 1247 data channels along the genome. Each table contained the number of specimens from each of the two groups that had either a loss, a gain, or no change at each data channel. We then tested whether there was a difference in the fre-

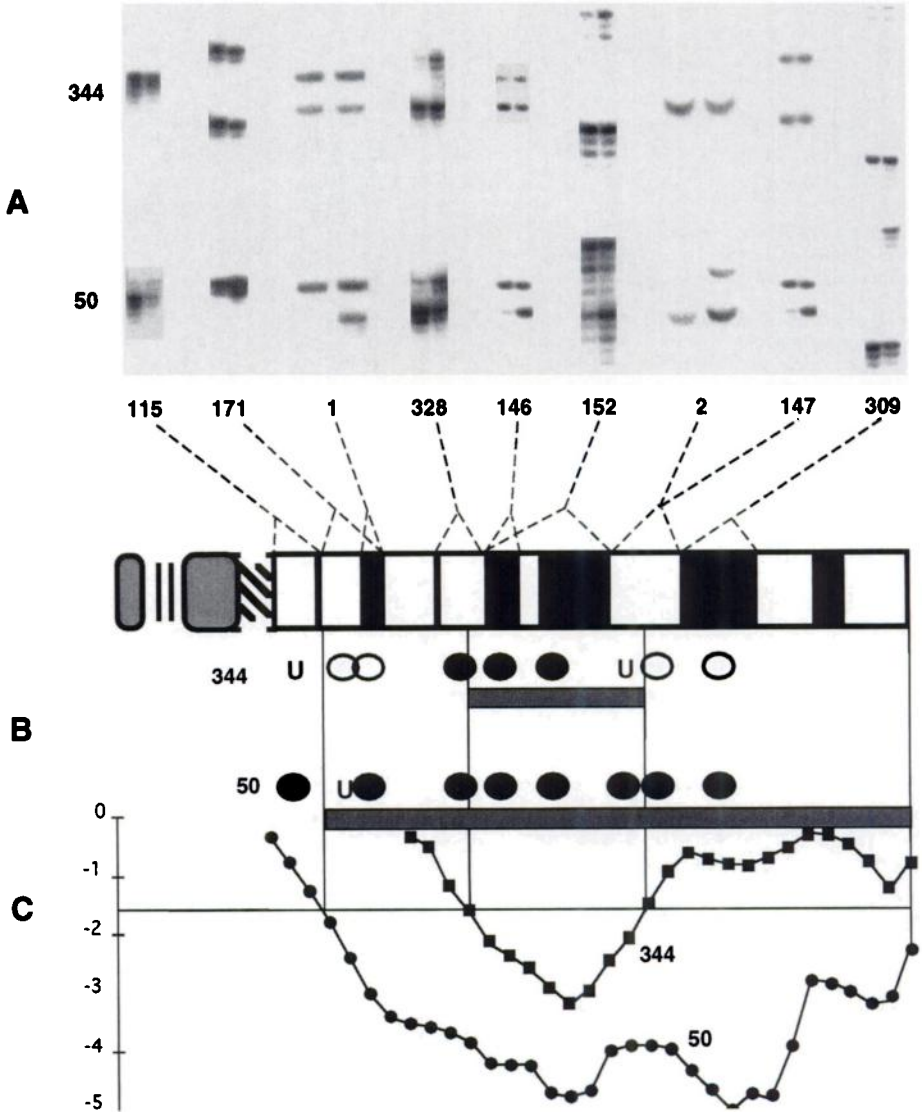

Fig. 4. Correlation of CGH and allelotyping data. Data from two representative tumors (tumors 50 and 344) are depicted. *A*, microsatellite and RFLP allelotyping at nine separate loci on chromosome 13q. For each case at each locus, autoradiograms of electrophoresis of PCR products from purified tumor DNA and paired noncancerous DNA from the same patient are shown in the *left* and *right lanes*, respectively. Mapped locations of each polymorphism (listed by D13S number) are indicated by the *dashed lines* leading to the *ideogram*. *B*, interpretation of allelotyping and CGH data. Allelotyping results are depicted as follows: ○, retained; ●, lost; and *U*, uninformative. The CGH interpretation for each tumor is shown by the *bar* indicating the length and position of deletions in each tumor with respect to the *ideogram*. For tumor 344, the physical locations of D13S147, D13S2, and D13S328 are not known precisely enough to define concordance with the termini of the CGH-defined deletion. Of the remaining five informative loci, all are concordant. The determinations for specimen 50 show seven polymorphisms that agree and one site (D13S115) showing LOH but $|t| < 1.6$. *C*, the calculated *t* statistics at each data channel. The *X axis* is drawn at $t = -1.6$, and the *vertical lines* connecting the *tracings* to the *ideogram* indicate the termini of the chromosome 13q losses found in these two tumors.

quency of gains or losses for each table using Fisher's exact test. The result of these analyses showed no more than the expected number of significant differences (at $P < 0.05$) based on performing a large number (1247) of tests.

Fig. 7 shows a summary of the frequency of gains and losses in regions of the genome that show alterations in many of the samples. None of the differences between the two groups is statistically significant ($P > 0.1$). One may conclude from these data that most chromosomal alterations occur without androgen-deprivation therapy.

Table 2 *Correlation of CGH findings with allelotyping results*

Results from the two techniques were compared[a] at each informative Southern or microsatellite locus.

	Allelotype result (Southern/Microsatellite)		
CGH result	Imbalance	Balance	Total
Loss or gain[b]	68	12	80
No alteration	6	150	156
Totals	74	162	236

[a] Applying the κ statistic (30); $\kappa = 0.83$ (0.70–0.95 is 95% confidence interval).
[b] In three of four instances of allelic imbalance on chromosome 8q, Southern analysis was able to detect a gain rather than a loss; by CGH, all alterations on chromosome 8qwere gains. All other allelic imbalances were losses by CGH.

Groups I and II Combined. Because the data sets for the two groups of tumors were not significantly different, we combined them and calculated the overall frequency of gain and loss at each channel (Fig. 7). For other subgroup comparisons of chromosomal alteration frequency, the combined data set was divided into groups based on younger or older patient age, higher or lower serum PSA, and ethnic group (African-American *versus* Caucasian). Similar contingency table analyses were carried out as described above. No regional differences in the frequency of gains or losses were detected among the groups defined by patient age or serum PSA.

In contrast, we did find an indication of increased frequency of gains in the region of 4q25-q28 in African-Americans. With a careful comparison of frequency histograms (such as those displayed in Figs. 5 and 6), this region was found to be the only one in which all five African-Americans showed an alteration. We found that the entire band 4q27 showed a significant gain in samples from 5 of 5 African-Americans as compared to 3 of 26 Caucasians. In addition, a larger region of six contiguous data channels in 4q27-q28 showed gain in at least 4 of 5 samples from African-Americans as compared to fewer than 4 of 26 samples from Caucasians (Fisher's exact $P < 0.01$ for

each comparison). We determined the statistical significance of this finding by randomly selecting subsets of 5 tumors, from among the total of 31, and repeating the contingency table analyses for the entire genome, each time comparing the subset of the randomly selected 5 with the remaining 26. We found that only 5% of these samples contained a section of six contiguous data channels with Fisher's exact $P < 0.01$ (based on 1000 randomly formed subsets). We also found that only 0.5% of theses randomly generated subsets showed "significant" gains on chromosome 4. In the comparison of African-Americans to Caucasians, no other regions in the genome differed significantly, although statistical power is low because of the small number of African-Americans in this study.

DISCUSSION

The goal of this study was to gain a pan-genomic view of the locations and frequencies of regional chromosomal alterations in prostate cancer. Genetic events leading to the initiation of prostate cancer are of obvious importance, but, because the majority of prostate cancers never metastasize (31), additional genetic events must be involved in the progression to lethal metastatic prostate cancer. By their proven ability to metastasize and their relative purity, the tumors studied here provided excellent material in which to define genetic alterations potentially involved in both initiation and progression of prostate cancer. Application of a new method for interpretation of fluorescence intensity values has led to a standardized CGH analysis, allowing detection and mapping of these genetic alterations based on statistical comparisons of intensity ratios relative to control experiments.

In 20 of the 31 cases studied, CGH analysis was corroborated with parallel Southern and microsatellite analysis of allelic imbalance on the same DNA. The good agreement between these two analytical techniques ($\kappa = 0.83$) provides assurance that the new, standardized CGH analysis is demonstrating high sensitivity and specificity.

Overall Genomic Considerations. The frequency of copy number alterations found in DNA samples from these advanced prostate cancer tissues seems rather large when viewed in light of flow cytometry and other ploidy studies, which have shown that metastatic prostate cancers are diploid in nearly 50% of the cases (32). However, the data presented here (Fig. 2) suggest that relatively equal proportions of the genome can be lost or gained, which may result in an overall balance of genetic material and a normal ploidy determination. In addition, when tumors are tetraploid, changes in copy number among different regions of the genome will be small relative to the total cellular DNA content. For example, tumor 399 was determined to be tetraploid on Feulgen staining and image analysis (data not shown). Thus, the losses and gains detected by CGH must be interpreted from a baseline of four allelic copies. Losses and gains were detected in approximately 5% and 18%, respectively, of the 1247 data channels across the genome. Although we were unable to determine exactly how many copies were lost or gained for each of the individual alterations, the data support the view that metastatic prostate cancers do contain critical DNA alterations that may not be detectable when measuring gross DNA content.

We also found that most regions of the genome are altered in at least 5% of advanced prostate cancer cases. These seemingly random alterations would not have been detected had they not been clonally present in a significant number of cells in the tissues from which DNA was extracted. We presume that chromosomal regions with low frequency of alteration occur as a result of random genomic instability of advanced cancer, and they probably do not contain genes important to the aggressive phenotype.

In the present study, gains were present as often as losses. However, the gains we detected were relatively low level in red:green fluorescence ratio and generally involved large regions or whole chromosome arms. We found no short, high-level amplifications suggestive of single oncogene amplification such as those described for breast cancer (33). Our results indicate a more subtle shift in gene copy numbers, which correlates with earlier reports on relatively low levels of amplification in prostate cancer (5, 10, 34, 35). It remains to be determined whether these frequent but low-level gains in copy number of specific chromosomal regions contribute to prostate cancer progression.

Regions of Loss. For this discussion, the combined data set of 31 advanced prostate cancers samples is being considered (Fig. 7). Regions of loss are suspected to carry at least one recessive oncogene; in fact, many of the most frequently lost regions contain known or candidate tumor suppressor genes. For example, the most intensively studied tumor suppressor gene, *p53*, is located on 17p and was shown previously to be mutated in 20–25% of metastatic prostate cancers (36). It also has been reported as mutated in 8 (50%) of 16 prostate cancer bone marrow metastases (37) and was shown to suppress *in vitro* growth of prostate cancer cell lines (38). Loss of 17p was detected in 50% of group I tumors as compared with 65% of group II tumors. These data taken together support the view that loss of normal p53 function is associated with prostate tumor progression, and it appears to be an alteration that occurs most commonly in late stages of the disease.

Chromosome 10q22.1–qter contains the candidate tumor suppressor gene *Mxi1*, reported previously to be mutated in four prostate cancer cases (39). Because the Mxi1 protein is suspected to repress c-Myc activity (40), loss of Mxi1 activity may lead to activation of c-Myc. In concert with potential increased chromosome 8q copy number (discussed below), increased c-Myc activity may be a common theme in prostate cancer.

Chromosome 5q contains the *α-catenin* gene (5q31; Ref. 41), which is a necessary component of the E-cadherin-mediated cell adhesion complex. It has been shown previously that five of the six human prostate cancer cell lines have reduced or absent levels of α-catenin or E-cadherin as compared with normal prostatic epithelial cells (42).

Two other frequently lost regions containing known candidate tumor suppressor genes are chromosome 13q (contains *Rb1*) and 16q (contains *E-cadherin*). Interestingly, close analysis of the patterns of loss on these chromosomal arms suggests that more than one important prostate cancer tumor suppressor gene may be located on 13q and 16q. Although the frequency of loss for all 31 tumors studied increases from 40 to 60% across 13q14, where *Rb1* is located, the peak appears just distal to 13q14 and is sustained near 60% across 13q21.1-q31 (see Figs. 5 and 6). Whereas previous studies have shown that loss of Rb1 expression (43) and allelic loss of this gene (44) do occur in prostate tumors, the CGH findings raise the possibility that there is a second important prostate cancer tumor suppressor gene on chromosome 13q distal to Rb1. Similarly, whereas decreased E-cadherin expression is associated with poor prognosis in prostate cancer (45, 46), and 30% of all 31 tumors in this study show loss in this region, there is a separate region of 40% loss at 16q24 that may signify the site of another important prostate cancer tumor suppressor gene. This regional mapping is in agreement with our previous cosmid deletion-mapping study on 16q (16). Further detailed analysis of these regions in a larger number of tumors is needed.

The other regions of frequent loss do not possess genes that have been identified previously as candidate tumor suppressor genes. However, the fact that these regions are lost at high frequency in advanced tumors indicates strongly that genes of importance to the progression of this disease may exist at these sites. In particular, there is great interest in the frequent loss of chromosome 8p, and a number of

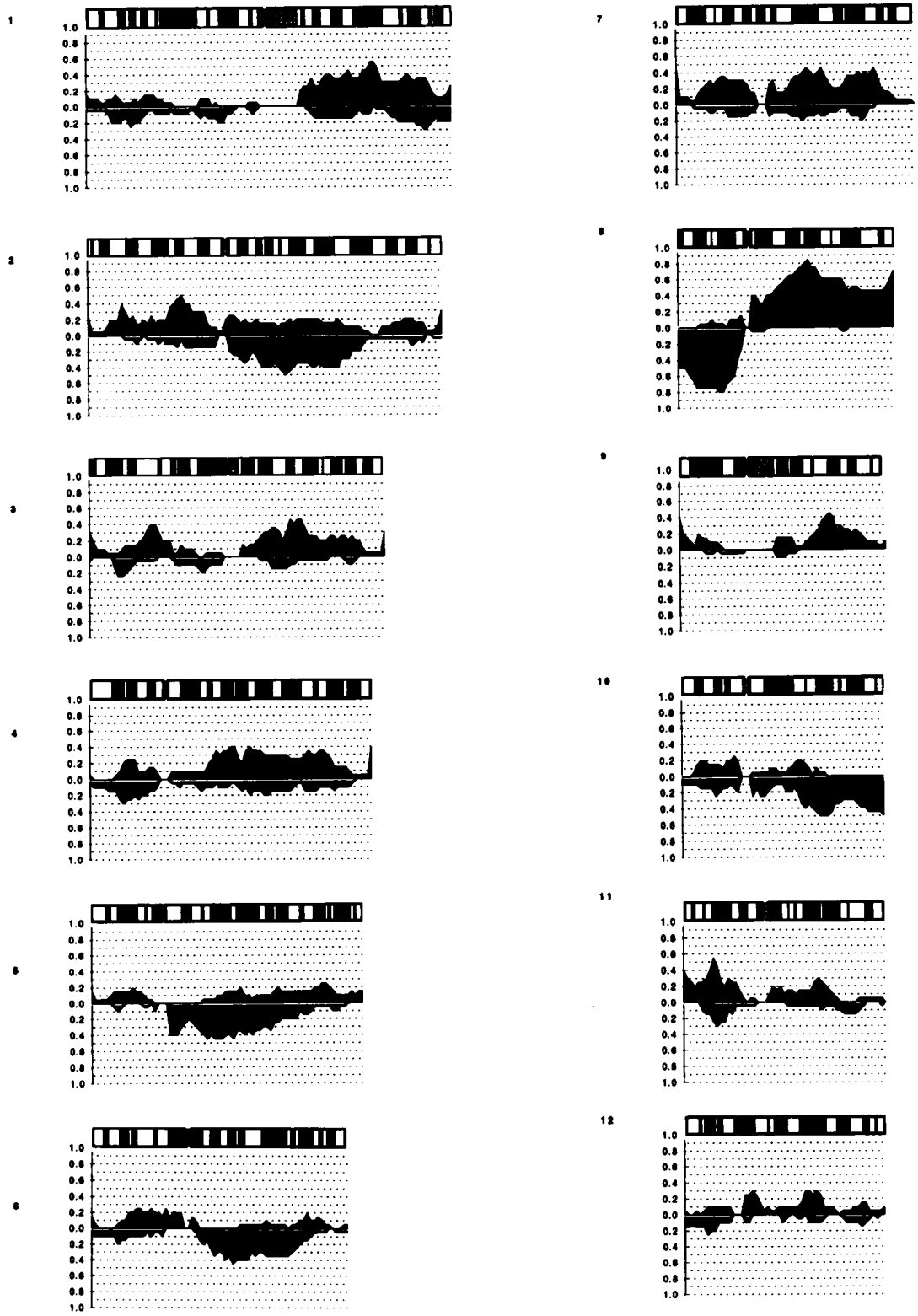

Fig. 5. Relative frequency histograms of genetic alterations in DNA from group I specimens. The relative frequency of gains and losses is shown as a region-specific histogram along each chromosome arm. The *Y* axis shows the proportion of specimens (of the 20 metastases analyzed) with $t > 1.6$ above the central axis and with $t < -1.6$ below the central axis. Centromeres and heterochromatic regions were excluded from analysis. Histograms are matched to ideograms of each chromosome based on the data channels, which contain the appropriate data distributed along the length of each chromosome. Chromosome identification numbers appear in the *upper left* of each *panel*.

research groups are investigating this region for the presence of an important tumor suppressor gene (10, 11, 13, 14, 22, 47). Regions 2q, 6q, 10p, and 15q also fall into this category and should be analyzed more extensively for such genes.

Regions of Gain. In these regions, we might expect to find dominant oncogenes that exhibit increased expression with increased copy number. The most notable of these is chromosome 8q, where the c-*Myc* oncogene is located. Amplification of this region was initially

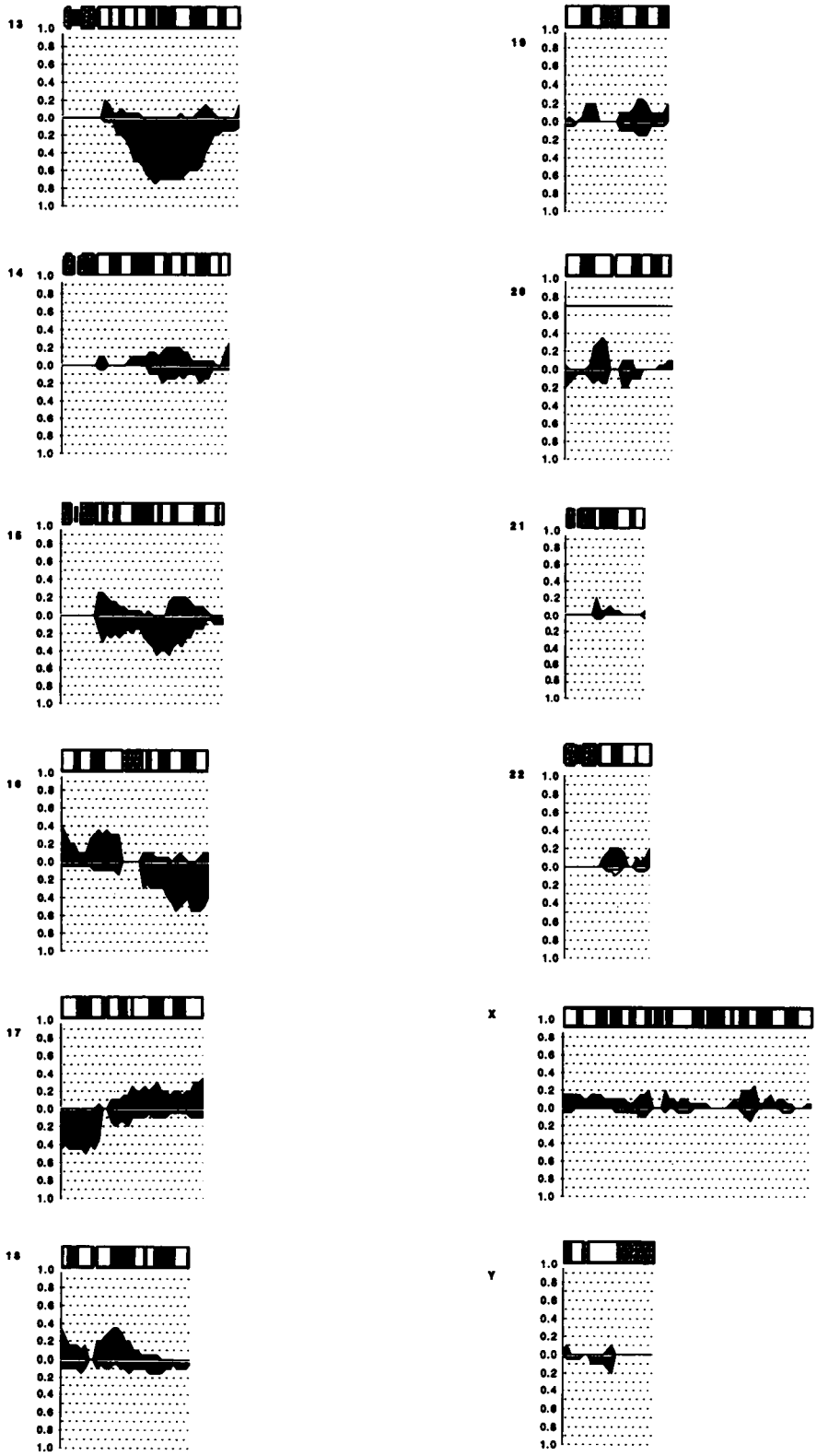

Fig. 5. *Continued.*

detected in prostate cancer by Southern analysis (10) and was shown subsequently to be correlated with adverse prognosis in prostate cancer (34). In the current study, we found a high frequency of 8q gains in both metastatic and recurrent primary tumors in patients with metastatic disease. This result is consistent with previous studies on recurrent tumors (23). Thus, c-Myc may play an important role in prostate cancer progression. However, we must note that *c-Myc* is located at 8q24, and the region of most common gain by CGH is 8q21.3 for both metastases and androgen-independent tumors. Thus, there may be another important oncogene in a region proximal to this known oncogene.

Chromosome 11p shows gains in 52% of the specimens in our

study, and the oncogene H-*Ras* is located at 11p15.5. Although this region is not identified as the most common region of gain (11p13-p15.3), CGH is unreliable near telomeres because of fluorescence intensity losses at the termini (see "Materials and Methods"). Thus, it may be that this oncogene is included in a region gained frequently in advanced prostate cancer. Notably, we determined that 40% (8/20) of the metastases show gains at 11p15.5 (see Fig. 5).

Another region that contains a known oncogene is chromosome 7p, where *erbB-1* (*epidermal growth factor receptor*) is located. Although it has been shown that trisomy in chromosome 7 is associated with higher grade and stage of prostate cancer (48, 49), no strong evidence has been published that indicates specific gene(s) on this chromosome that are important to the phenotype.

Fig. 7 shows that chromosome 7q displays gains in up to 40% of the specimens from both the metastases and the androgen-independent tumors. Recently, it has been shown that the c-*met* oncogene, which maps to 7q31, is expressed in the basal epithelial cells of 36 of 43 primary prostate cancer samples, 4 of 4 lymph node metastases, and 23 of 23 bone marrow metastases (50).

Fig. 7 indicates that gains occur at a frequency of 0.39 in a region of chromosome 17q that includes *BRCA1*, whereas Gao *et al.* (51) recently showed frequent PCR-based LOH of BRCA1 on chromosome 17q in prostate cancer. These results could be explained by somatic recombination (resulting in LOH) followed by gain, or incorrect interpretation of PCR allelic bands. Future study should resolve these inconsistencies.

The oncogene *erbB*-2 is located at 17q12, which is in the vicinity of the region of high frequency of gain by CGH. Previously, Kuhn *et al.* (52) have shown that 18 of 53 clinically localized prostate cancers expressed high levels of this gene with no indications of high-level gene amplification. It is possible that the modest increase in copy number that is evident in our analyses is responsible for such increased gene expression.

The androgen receptor gene, located in Xq12, was shown previously to display gains at a relatively high frequency (four of nine) in recurrent prostate tumors (23). In a subsequent report, Visakorpi *et al.* (5) showed that amplification of Xq12 is associated with tumor recurrence in individuals during androgen deprivation therapy. Although this region was gained in only 5 (16%) of our entire group of 31 tumors, it was gained in 3 (27%) of 11 of the group II androgen

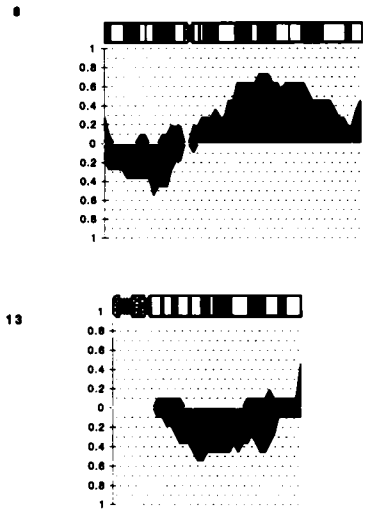

Fig. 6. Frequency histograms of chromosomal alterations in group II specimens. Examples of frequency histograms for the two chromosomes most frequently altered in group II specimens are shown for comparison to group I (see Fig. 5). The frequency of gains and losses are depicted as described in Fig. 5.

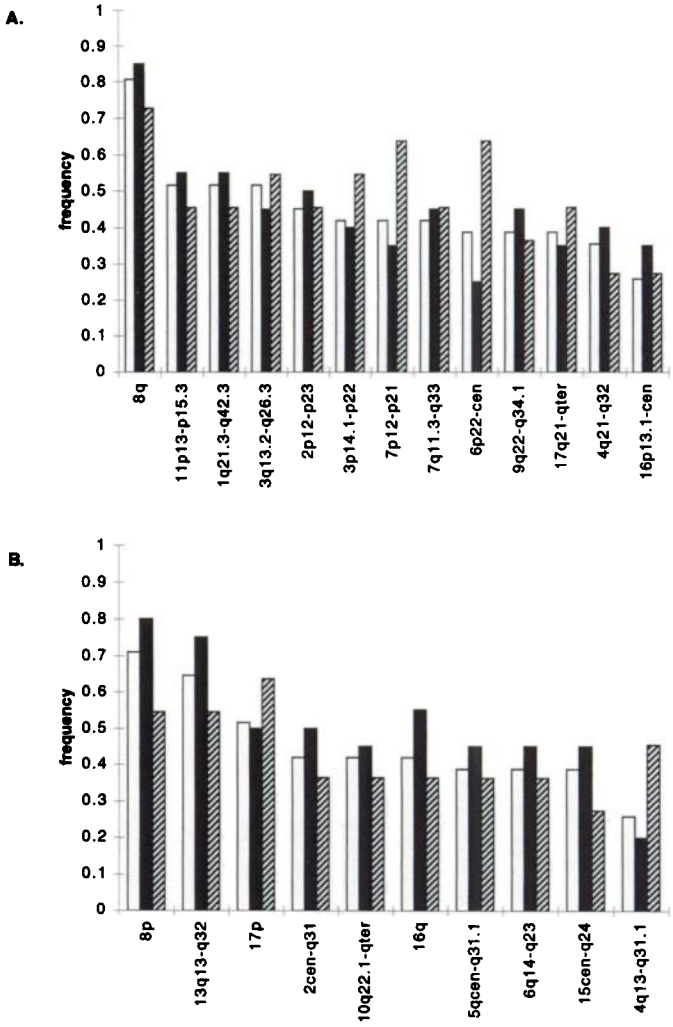

Fig. 7. Maximum frequency of alteration of any data channel within most frequently altered regions: *white bars*, entire group; *black bars*, group I; and *hatched bars*, group II. Regions are defined as a minimum of five contiguous channels in which a significant alteration ($|r| > 1.6$) is found for greater than 20% of the samples. *A*, gains. *B*, losses.

independent tumors. Thus, our studies are in general agreement with those of Visakorpi *et al.* (5) and support their suggestion that tumor cells with androgen receptor amplification are selected during androgen deprivation therapy. However, amplification of this region is not restricted to tumors failing hormonal therapy.

African-Americans. Our finding of increased frequency of gains in the region 4q25-q28 in African-Americans ($P < 0.001$) is provocative. Perhaps there exists a gene located on 4q that is more frequently increased in activity and induces more rapid clinical progression of prostate cancer among African-Americans (53, 54). In any case, our data demonstrate that the pattern of genetic alterations in tumors from African-Americans is largely the same as that seen in tumors from Caucasians. Studies with larger numbers of patients must be performed to determine fully any significant molecular genetic differences.

Summary. A new quantitative statistical method of comparative genomic hybridization, corroborated by microsatellite and Southern analysis of allelic imbalance, has been used to identify several novel regions of frequent deletion or gain of DNA copy numbers in prostate cancer, and has helped to clarify the relative importance of several other previously reported regions of loss or gain. Modified function of genes contained within the most frequently altered regions may be largely responsible for the malignant behavior of prostate cancer.

Additional study of these genomic regions may provide critical insight into the mechanism of prostate cancer progression and may generate important tools for better tumor-specific prognosis and treatment of prostate cancer.

ACKNOWLEDGMENTS

We give special thanks to Dr. Patrick C. Walsh, Dr. Charles Brendler, Dr. Fray F. Marshall, Dr. Jacek Mostwin, Dr. Louis R. Kavoussi, Dr. Robert G. Moore, Dr. Harold Alfert, and Dr. Frank J. Frassica of The Johns Hopkins University (Baltimore, MD) and Dr. Natasha Kyprianou, Dr. Stephen C. Jacobs, and Dr. Geoffrey N. Sklar of The University of Maryland (Baltimore, MD) for critical assistance in obtaining tissue for this study. In addition, we thank Damir Sudar, Dr. James Piper, and Vikas Chhabra for developing the hardware and software for CGH and assisting in its application at the University of California, San Francisco, as well as Piroska Bujnovszky for laboratory assistance at The Johns Hopkins University.

REFERENCES

1. Friend, S. H., Bernards, R., Rogelj, S., Weinberg, R. A., Rapaport, J. M., Albert, D. M., and Dryja, T. P. A human DNA segment with properties of the gene that predisposes to retinoblastoma and osteosarcoma. Nature (Lond.), *323:* 643–646, 1986.
2. Cawthon, R. M., Weiss, R., Gangfeng, X., Viskochil, D., Culver, M., Stevens, J., Robertson, M., Dunn, D., Gesterland, R., O'Connell, P., and White, R. A major segment of the *neurofibromatosis type 1* gene: cDNA sequence, genomic structure, and point mutations [Published erratum appears in Cell 1990 Aug 10;62: after p. 608]. Cell, *62:* 193–201, 1990.
3. Baker, S. J., Fearon, E. R., Nigro, J. M., Hamilton, S. R., Preisinger, A. C., Jessup, J. M., vanTuinen, P., Ledbetter, D. H., Barker, D. F., Nakamura, Y., White, R., and Vogelstein, B. Chromosome 17 deletions and *p53* gene mutations in colorectal carcinomas. Science (Washington DC), *244:* 217–221, 1989.
4. Shuin, T., Kondo, K., Torigoe, S., Kishida, T., Kubota, Y., Hosaka, M., Nagashima, Y., Kitamura, H., Latif, F., Zbar, B., Lerman, M. I., and Yao, M. Frequent somatic mutations and loss of heterozygosity of the von Hippel-Lindau tumor suppressor gene in primary human renal cell carcinomas. Cancer Res., *54:* 2852–2855, 1994.
5. Visakorpi, T., Hyytinen, E., Koivisto, P., Tanner, M., Keinanen, R., Palmberg, C., Palotie, A., Tammela, T., Isola, J., and Kallioniemi, O-P. *In vivo* amplification of the androgen receptor gene and progression of human prostate cancer. Nat. Genet., *9:* 401–406, 1995.
6. Jen, J., Kim, H., Piantadosi, S., Liu, Z. F., Levitt, R. C., Sistonen, P., Kinzler, K. W., Vogelstein, B., and Hamilton, S. R. Allelic loss of chromosome 18q and prognosis in colorectal cancer. N. Engl. J. Med., *331:* 213–221, 1994.
7. Grundy, P. E., Telzerow, P. E., Breslow, N., Moksness, J., Huff, V., and Paterson, M. C. Loss of heterozygosity for chromosomes 16q and 1p in Wilms' tumors predicts an adverse outcome. Cancer Res., *54:* 2331–2333, 1994.
8. Carter, B. S., Ewing, C. M., Ward, W. S., Treiger, B. F., Aalders, T. W., Schalken, J. A., Epstein, J. I., and Isaacs, W. B. Allelic loss of chromosomes 16q and 10q in human prostate cancer. Proc. Natl. Acad. Sci. USA, *87:* 8751–8755, 1990.
9. Kunimi, K., Bergerheim, U. S., Larsson, I. L., Ekman, P., and Collins, V. P. Allelotyping of human prostatic adenocarcinoma. Genomics, *11:* 530–536, 1991.
10. Bova, G. S., Carter, B. S., Bussemakers, M. J., Emi, M., Fujiwara, Y., Kyprianou, N., Jacobs, S. C., Robinson, J. C., Epstein, J. I., Walsh, P. C., and Isaacs, W. B. Homozygous deletion and frequent allelic loss of chromosome 8p22 loci in human prostate cancer. Cancer Res., *53:* 3869–3873, 1993.
11. MacGrogan, D., Levy, A., Bostwick, D., Wagner, M., Wells, D., and Bookstein, R. Loss of chromosome 8p loci in prostate cancer: mapping by quantitative allelic imbalance. Genes Chromosomes & Cancer, *10:* 151–159, 1994.
12. Bergerheim, U. S., Kunimi, K., Collins, V. P., and Ekman, P. Deletion mapping of chromosomes 8, 10, and 16 in human prostatic carcinoma. Genes Chromosomes & Cancer, *3:* 215–220, 1991.
13. Chang, M., Tsuchiya, K., Batchelor, R. H., Rabinovitch, P. S., Kulander, B. G., Haggitt, R. C., and Burmer, G. C. Deletion mapping of chromosome 8p in colorectal carcinoma and dysplasia arising in ulcerative colitis, prostatic carcinoma, and malignant fibrous histiocytomas. Am. J. Pathol., *144:* 1–6, 1994.
14. Trapman, J., Sleddens, H. F., vanderWeiden, M. M., Dinjens, W. N., Konig, J. J., Schroder, F. H., Faber, P. W., and Bosman, F. T. Loss of heterozygosity of chromosome 8 microsatellite loci implicates a candidate tumor suppressor gene between the loci *D8S87* and *D8S133* in human prostate cancer. Cancer Res., *54:* 6061–6064, 1994.
15. Suzuki, H., Emi, M., Komiya, A., Fujiwara, Y., Yatani, R., Nakamura, Y., and Shimazaki, J. Localization of a tumor suppressor gene associated with progression of human prostate cancer within a 1.2 mb region of 8p22–p21.3. Genes Chromosomes & Cancer, *13:* 168–174, 1995.
16. Cher, M. L., Ito, T., Weidner, N., Carroll, P. R., and Jensen, R. H. Mapping of regions of physical deletion on chromosome 16q in prostate cancer cells by fluorescence *in situ* hybridization (FISH). J. Urol., *153:* 249–254, 1995.
17. Phillips, S. M., Morton, D. G., Lee, S. J., Wallace, D. M., and Neoptolemos, J. P. Loss of heterozygosity of the retinoblastoma and adenomatous polyposis susceptibility gene loci and in chromosomes 10p, 10q and 16q in human prostate cancer. Br. J. Urol., *73:* 390–395, 1994.
18. Sakr, W. A., Macoska, J. A., Benson, P., Grignon, D. J., Wolman, S. R., Pontes, J. E., and Crissman, J. D. Allelic loss in locally metastatic, multisampled prostate cancer. Cancer Res., *54:* 3273–3277, 1994.
19. Latil, A., Baron, J. C., Cussenot, O., Fournier, G., Soussi, T., Boccon, G. L., Le, D. A., Rouesse, J., and Lidereau, R. Genetic alterations in localized prostate cancer: identification of a common region of deletion on chromosome arm 18q. Genes Chromosomes & Cancer, *11:* 119–125, 1994.
20. Massenkeil, G., Oberhuber, H., Hailemariam, S., Sulser, T., Diener, P. A., Bannwart, F., Schafer, R., and Schwarte, W. I. P53 mutations and loss of heterozygosity on chromosomes 8p, 16q, 17p, and 18q are confined to advanced prostate cancer. Anticancer Res., *14:* 2785–2790, 1994.
21. Kallioniemi, A., Kallioniemi, O. P., Sudar, D., Rutovitz, D., Gray, J. W., Waldman, F., and Pinkel, D. Comparative genomic hybridization for molecular cytogenetic analysis of solid tumors. Science (Washington DC), *258:* 818–821, 1992.
22. Cher, M. L., MacGrogan, D., Bookstein, R., Brown, J. A., Jenkins, R. B., and Jensen, R. H. Comparative genomic hybridization, allelic imbalance, and FISH on chromosome 8 in prostate cancer. Genes Chromosomes & Cancer, *11:* 153–162, 1994.
23. Visakorpi, T., Kallioniemi, A. H., Syvanen, A., Hyytinen, E. R., Karhu, R., Tammela, T., Isola, J. J., and Kallioniemi, O-P. Genetic changes in primary and recurrent prostate cancer by comparative genomic hybridization. Cancer Res., *55:* 342–347, 1995.
24. Gleason, D. F. Classification of prostatic carcinomas. Cancer Chemother. Rep., *50:* 125–128, 1966.
25. Kallioniemi, O. P., Kallioniemi, A., Piper, J., Isola, J., Waldman, F. M., Gray, J. W., and Pinkel, D. Optimizing comparative genomic hybridization for analysis of DNA sequence copy number changes in solid tumors. Genes Chromosomes & Cancer, *10:* 231–243, 1994.
26. Morton, N. E. Parameters of the human genome. Proc. Natl. Acad. Sci. USA, *88:* 7474–7476, 1991.
27. Lucas, J. N., and Gray, J. W. Centromeric index *versus* DNA content flow karyotypes of human chromosomes measured by means of slit-scan flow cytometry. Cytometry, *8:* 273–279, 1987.
28. Moore, D. H. I., Cher, M. L., and Gray, J. W. A *t*-statistic for objective interpretation of comparative genomic hybridization (CGH) profiles. Cytometry, in press, 1996.
29. Weissenbach, J., Gyapay, G., Dib, C., Vignal, A., Morissette, J., Millasseau, P., Vaysseix, G., and Lathrop, M. A second-generation linkage map of the human genome. Nature (Lond.), *359:* 794–801, 1992.
30. Cohen, J. A coefficient of agreement for nominal scales. Educ. Psychol. Meas., *20:* 37–46, 1960.
31. Dhom, G. Epidemiologic aspects of latent and clinically manifest carcinoma of the prostate. J. Cancer Res. Clin. Oncol., *106:* 210–218, 1983.
32. Stephenson, R. A., James, B. C., Gay, H., Fair, W. R., Whitmore, W. J., and Melamed, M. R. Flow cytometry of prostate cancer: relationship of DNA content to survival. Cancer Res., *47:* 2504–2507, 1987.
33. Kallioniemi, A., Kallioniemi, O. P., Piper, J., Tanner, M., Stokke, T., Chen, L., Smith, H. S., Pinkel, D., Gray, J. W., and Waldman, F. M. Detection and mapping of amplified DNA sequences in breast cancer by comparative genomic hybridization. Proc. Natl. Acad. Sci. USA, *91:* 2156–2160, 1994.
34. Van Den Berg, C., Guan, X., Von Hoff, D., Jenkins, R., Bittner, M., Griffin, C., Kallioniemi, O., Visakorpi, T., McGill, J., Herath, J., Epstein, J., Sarosdy, M., Meltzer, P., and Trent, J. DNA sequence amplification in human prostate cancer identified by chromosome microdissection: potential prognostic implications. Clin. Cancer Res., *1:* 11–18, 1995.
35. Brothman, A. R., Peehl, D. M., Patel, A. M., and McNeal, J. E. Frequency and pattern of karyotypic abnormalities in human prostate cancer. Cancer Res., *50:* 3795–3803, 1990.
36. Bookstein, R., MacGrogan, D., Hilsenbeck, S. G., Sharkey, F., and Allred, D. C. p53 is mutated in a subset of advanced-stage prostate cancers. Cancer Res., *53:* 3369–3373, 1993.
37. Aprikian, A. G., Sarkis, A. S., Fair, W. R., Zhang, Z. F., Fuks, Z., and Cordon-Cardo, C. Immunohistochemical determination of p53 protein nuclear accumulation in prostatic adenocarcinoma. J. Urol., *151:* 1276–1280, 1994.
38. Isaacs, W. B., Carter, B. S., and Ewing, C. M. Wild-type p53 suppresses growth of human prostate cancer cells containing mutant p53 alleles. Cancer Res., *51:* 4716–4720, 1991.
39. Eagle, L. R., Yin, X., Brothman, A. R., Williams, B. J., Atkin, N. B., and Prochownik, E. V. Mutation of the *MXI1* gene in prostate cancer. Nat. Genet., *9:* 249–255, 1995.
40. Zervos, A. S., Gyuris, J., and Brent, R. Mxi1, a protein that specifically interacts with Max to bind Myc-Max recognition sites. Cell, *72:* 223–232, 1993.
41. Furukawa, Y., Nakatsuru, S., Nagafuchi, A., Tsukita, S., Muto, T., Nakamura, Y., and Horii, A. Structure, expression and chromosome assignment of the human catenin (cadherin-associated protein) α1 gene (CTNNA1). Cytogenet. Cell Genet., *65:* 74–78, 1994.
42. Morton, R. A., Ewing, C. M., Nagafuchi, A., Tsukita, S., and Isaacs, W. B. Reduction of E-cadherin levels and deletion of the α-catenin gene in human prostate cancer cells. Cancer Res., *53:* 3585–3590, 1993.
43. Bookstein, R., Rio, P., Madreperla, S. A., Hong, F., Allred, C., Grizzle, W. E., and Lee, W. H. Promoter deletion and loss of retinoblastoma gene expression in human prostate carcinoma. Proc. Natl. Acad. Sci. USA, *87:* 7762–7766, 1990.
44. Brooks, J. D., Bova, G. S., and Isaacs, W. B. Allelic loss of the retinoblastoma gene in primary human prostatic adenocarcinomas. Prostate, *26:* 35–39, 1995.
45. Umbas, R., Isaacs, W. B., Bringuier, P. P., Schaafsma, H. E., Karthaus, H. F., Oosterhof, G. O., Debruyne, F. M., and Schalken, J. A. Decreased E-cadherin expression is associated with poor prognosis in patients with prostate cancer. Cancer Res., *54:* 3929–3933, 1994.

46. Umbas, R., Schalken, J. A., Aalders, T. W., Carter, B. S., Karthaus, H. F., Schaafsma, H. E., Debruyne, F. M., and Isaacs, W. B. Expression of the cellular adhesion molecule E-cadherin is reduced or absent in high-grade prostate cancer. Cancer Res., *52:* 5104–5109, 1992.
47. Matsuyama, H., Pan, Y., Skoog, L., Tribukait, B., Naito, K., Ekman, P., Lichter, P., and Bergerheim, U. S. Deletion mapping of chromosome 8p in prostate cancer by fluorescence *in situ* hybridization. Oncogene, *9:* 3071–3076, 1994.
48. Bandyk, M. G., Zhao, L., Troncoso, P., Pisters, L. L., Palmer, J. L., von Eschenbach, A. C., Chung, L. W., and Liang, J. C. Trisomy 7: a potential cytogenetic marker of human prostate cancer progression. Genes Chromosomes & Cancer, *9:* 19–27, 1994.
49. Alcaraz, A., Takahashi, S., Brown, J. A., Herath, J. F., Bergstralh, E. J., Larson, K. J., Lieber, M. M., and Jenkins, R. B. Aneuploidy and aneusomy of chromosome 7 detected by fluorescence *in situ* hybridization are markers of poor prognosis in prostate cancer. Cancer Res., *54:* 3998–4002, 1994.
50. Pisters, L. L., Troncoso, P., Zhau, H. E., Li, W., von, E. A., and Chung, L. W. c-*met* proto-oncogene expression in benign and malignant human prostate tissues. J. Urol., *154:* 293–298, 1995.
51. Gao, X., Zacharek, A., Salkowski, A., Grignon, D. J., Sakr, W., Porter, A. T., and Honn, K. V. Loss of heterozygosity of the *BRCA1* and other loci on chromosome 17q in human prostate cancer. Cancer Res., *55:* 1002–1005, 1995.
52. Kuhn, E. J., Kurnot, R. A., Sesterhenn, I. A., Chang, E. H., and Moul, J. W. Expression of the c-erbB-2 (HER-2/neu) oncoprotein in human prostatic carcinoma (Review). J. Urol., *150:* 1427–1433, 1993.
53. Pienta, K. J., Demers, R., Hoff, M., Kau, T. Y., Montie, J. E., and Severson, R. K. Effect of age and race on the survival of men with prostate cancer in the Metropolitan Detroit tricounty area, 1973 to 1987. Urology, *45:* 93–102, 1995.
54. Brawn, P. N., Johnson, E. H., Kuhl, D. L., Riggs, M. W., Speights, V. O., Johnson, C. F., Pandya, P. P., Lind, M. L., and Bell, N. F. Stage at presentation and survival of white and black patients with prostate carcinoma. Cancer (Phila.), *71:* 2569–2573, 1993.